



Scaling and analysis of mixing in large stratified volumes

P. F. PETERSON

Department of Nuclear Engineering, University of California, Berkeley, CA 94720, U.S.A.

Abstract—This work develops scaling and governing equations for mixing processes in large interconnected enclosures under stratified conditions. Injected buoyant jets, plumes from heat sources, and wall jets from heat transfer to structures can generate such mixing. Using the hierarchical two-tiered scaling analysis method, criteria are developed for the prediction of ambient enclosure fluid stratification due to temperature and/or concentration gradients. Simplified governing equations for mass, energy, and species conservation result. In their simplified form, the governing equations allow both scaling and simplified modeling and analysis of integral system behavior. The application to numerical analysis of mixing is illustrated with an example related to nuclear reactor containment mixing.

1. INTRODUCTION

MASS, ENERGY and species transport in large interconnected enclosures is of interest in a variety of applications, including nuclear reactor containments, building fires, HVAC systems, chemical processing, and pollutant dispersal. The important transport mechanisms are often characterized by time and length scales which can differ by orders of magnitude, from low velocity convection in large stratified or stagnant regions to high velocity flows in thin jets. Often strong stratification is observed in large enclosures, induced by temperature and/or concentration gradients. Inside stably stratified enclosures, jets become the primary source of vertical mixing, both wall jets created by natural convection boundary layers and free jets generated by injected fluids or heat sources.

When strongly stratified, an enclosure's ambient temperature and concentration distributions can be considered one-dimensional, with negligible horizontal gradients except in narrow regions occupied by jets. Jaluria and coworkers [1–3] have exploited the one dimensional temperature distribution to develop zone mixing models for enclosure fires. Under zone mixing, the ambient enclosure temperature distribution is divided into a hot ceiling layer and cool floor layer divided by a sharp horizontal interface. Mixing between the regions is then generated by buoyant plumes from fires and by wall jets which form on cold structure surfaces. Fox *et al.* [4] and Smith *et al.* [5] found that experimental results for transient stratification of boiling water reactor (BWR) pressure suppression pools could also be predicted using numerical solutions of ordinary differential equations describing the effect of buoyant jets on the vertical temperature distribution. Peterson *et al.* [6] showed that convenient scaling parameters for design of

scaled experiments for reactor containment simulation can be derived for stratified conditions.

Both scaling and modeling of stratified mixing in large enclosures require detailed and accurate empirical models for wall and free jets. Considerable research has been devoted to the study of transport by jets, plumes, and wall boundary layers in large-scale stratified systems. Strong stratification is commonly found in ecological systems, both air and water bodies, where jet and plume dispersal of pollutants such as smoke stack and sewage discharges are of interest. Several useful general references are available for mixing by free buoyant jets in stratified and unstratified environments [7–9]. Entrainment into wall jets can also be treated using integral methods [1–3].

This work derives governing equations for mixing of stratified fluids in large enclosures. The hierarchical, two-tiered scaling analysis (HTTSA) method, presented by Zuber [10], is applied. The scaling process results in nondimensional parameters which govern when the onset and breakdown of ambient stratification occurs for enclosure flows driven by wall and free jets. The parameter for forced jets is shown to correlate existing data for stratification breakdown by free buoyant jets in shallow fluid layers. An application of the governing equations to numerical analysis is then presented.

2. HIERARCHICAL SCALING

The individual transport mechanisms which govern mixing in large volumes are characterized by time and length scales which can differ by orders of magnitude. In large-scale systems, the complexity of the interactions of the various transport mechanisms can make analysis, numerical modeling and experimental simulation a daunting task. For this reason Zuber [10]

NOMENCLATURE

<p><i>A</i> area</p> <p><i>B</i> buoyancy flux</p> <p><i>c</i> specific heat</p> <p><i>C</i> constant, equation (41)</p> <p><i>d</i> diameter</p> <p><i>D</i> mass diffusion coefficient</p> <p>e_z vertical unit vector</p> <p>F vector of fluxes</p> <p><i>g</i> gravitational acceleration</p> <p>G vector of conserved quantities</p> <p><i>Gr</i> Grashof number</p> <p><i>H</i> height</p> <p><i>i</i> enthalpy</p> <p><i>k</i> thermal conductivity</p> <p>k_m, k_μ entrainment coefficients</p> <p><i>m</i> mass, exponent/number of vertical nodes</p> <p><i>M</i> momentum</p> <p><i>n</i> number of jets</p> <p><i>ns</i> number of species/phases</p> <p>n unit normal vector</p> <p><i>p</i> perimeter</p> <p><i>P</i> pressure</p> <p><i>Pr</i> Prandtl number</p> <p><i>q</i> power</p> <p><i>Q</i> volume flow rate</p> <p><i>Re</i> Reynolds number</p> <p><i>Ri</i> Richardson number</p> <p><i>S</i> surface</p> <p>S vector of source terms</p> <p><i>t</i> time</p> <p><i>T</i> temperature</p> <p>u_c jet entrainment velocity</p> <p>u mass average velocity vector</p>	<p><i>U</i> velocity</p> <p><i>V</i> volume</p> <p><i>x</i> horizontal coordinate</p> <p><i>y</i> horizontal coordinate</p> <p><i>z</i> vertical coordinate.</p> <p style="text-align: center;">Greek symbols</p> <p>α_T Taylor's jet entrainment constant</p> <p>β thermal expansion coefficient</p> <p>δ boundary layer thickness, Kroneker delta</p> <p>θ nondimensional temperature</p> <p>μ dynamic viscosity</p> <p>ν kinematic viscosity</p> <p>Π specific or characteristic time ratio</p> <p>ρ density</p> <p>τ residence time</p> <p>χ mass fraction</p> <p>ω specific frequency.</p> <p style="text-align: center;">Subscripts</p> <p>a ambient</p> <p>bj free buoyant jet</p> <p>bl wall jet (boundary layer)</p> <p>e entrainment</p> <p><i>j</i> index number</p> <p><i>k</i> index number</p> <p>o entrance/nominal value</p> <p>sf ambient, stratified fluid.</p> <p style="text-align: center;">Superscripts</p> <p>s specific (for a well defined geometry)</p> <p>+</p>
--	--

presented a hierarchical, two-tiered scaling analysis to provide a convenient and self-consistent method for ranking the importance of transport processes in a specific system, and for specifying the required level of detail for the analysis and scaling of the processes. For illustration of HTTSA the specific problem of nuclear reactor containment analysis is examined here, however, the results are easily generalized to other systems.

Light water reactor (LWR) containment systems typically consist of large volumes interconnected with pipes, channels, or doors. Pressure differentials drive transport between the volumes. Following a loss of coolant accident (LOCA) steam generated in the reactor pressure vessel by decay heat can vent into the containment structure. The transport and condensation of the steam is strongly affected by its mixing with the ambient noncondensable gas. Due to the large differences between the molecular weights of water vapor and air/nitrogen, and the typical differences in their temperatures, large density differences

can exist between the injected buoyant jet fluid and the ambient enclosure fluid. Based on criteria presented here, at later periods of a LOCA, strong stratification can be expected in the gas spaces of passive containment systems. Stratification in BWR pressure suppression pools remains important throughout an accident. The transport of hydrogen and aerosols also become of interest in the case of severe accidents with fuel damage.

The HTTSA method divides a complex system into subsystems, modules, constituents, and phases. For the application to mixing in and between large enclosures, individual enclosures and interconnecting channels between enclosures can be selected as subsystems, as illustrated in Fig. 1. Within each subsystem modules are defined. The large enclosures are divided into liquid pool and gas space modules, as appropriate. The constituent materials of each module are then, for a typical LWR containment, water, noncondensable gas (air or nitrogen), aerosol particulates, steel, and concrete. The primary phases are liquid

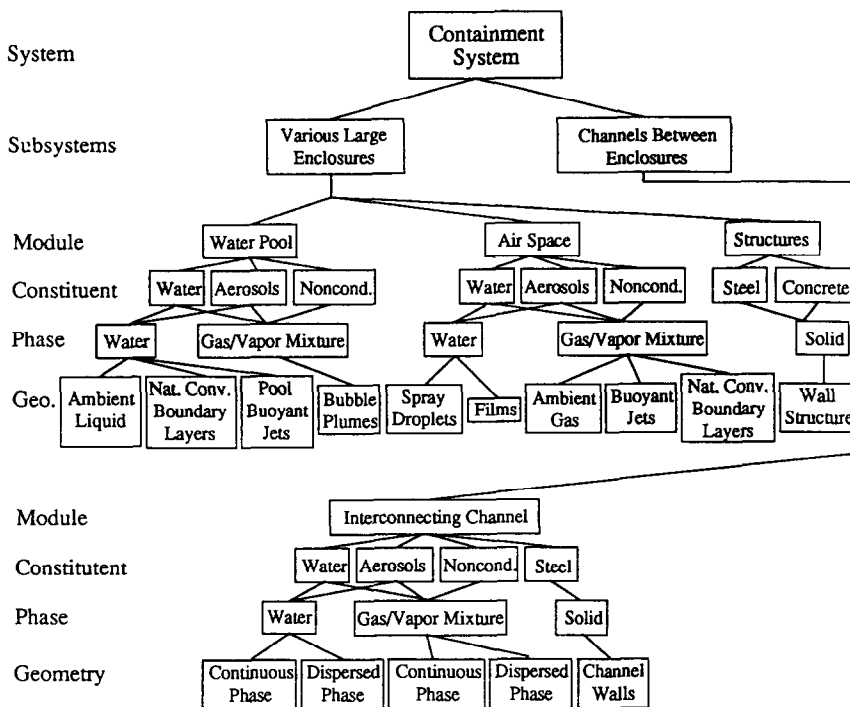


FIG. 1. Hierarchical scaling for large interconnected LWR enclosures.

water, gas/water vapor mixtures, and solids. Each phase can exist in several geometrical configurations, such as droplets, films, and bubbles, or as a continuous phase. This work defines free jets, wall jets, and ambient fluid as the primary phase geometries in large enclosures. For each geometrical configuration of a phase, there exist fields which describe the distribution of mass, momentum, energy, and species, which may vary with time. Each field is governed by conservation requirements and by transport processes which can be characterized by a length scale (the specific area) and a time scale (a rate).

Two time constants are calculated for each geometrical configuration. The specific frequency (for well defined geometry) or characteristic frequency is defined as the ratio of the rate of mass, momentum, energy, or species transport into the geometry volume, to the capacity of the volume to store the mass, momentum, energy, or species. The specific frequencies for free buoyant jets, ω_{bj}^s , and natural convection wall jets, ω_{bl}^s , and the characteristic frequency for the ambient fluid, ω_{sf} , are

$$\omega_{bj}^s = \frac{u_e A_{bj}}{V_{bj}} \quad \omega_{bl}^s = \frac{u_e A_{bl}}{V_{bl}}$$

$$\omega_{sf} = \frac{\sum_{k=1}^n u_{ek} A_k}{V_{sf}} \quad (1)$$

where u_e is the characteristic entrainment velocity over the jet surface area A , V the volume occupied by the phase geometry, and n the number of free or wall jets.

The second time constant is the residence time, τ , the ratio of the volume occupied by the geometrical configuration V and the characteristic volume flow rate into the configuration Q_o . The residence times for fluid in free buoyant jets, τ_{bj}^s , natural convection wall jets, τ_{bl}^s , and ambient fluid, τ_{sf} , are

$$\tau_{bj}^s = \frac{n_{bj} V_{bj}}{Q_o} \quad \tau_{bl}^s = \frac{n_{bl} V_{bl}}{Q_o} \quad \tau_{sf} = \frac{V_{sf}}{Q_o} \quad (2)$$

Because flow in ambient fluid is generated primarily by entrainment into walls and free jets, the same characteristic volume flow rate Q_o is used for each geometry.

When fluid residence times in one phase geometry are short compared to residence in another, then the detailed transient distribution of mass, energy, and species in that phase geometry become unimportant, and only the integral, quasi-steady, time averaged behavior requires consideration. When residence times in the ambient fluid are large compared to residence times in the free and wall jets, that is

$$\frac{\tau_{sf}}{\tau_{bj}^s} = \frac{V_{sf}}{n_{bj} V_{bj}} \gg 1 \quad \frac{\tau_{sf}}{\tau_{bl}^s} = \frac{V_{sf}}{n_{bl} V_{bl}} \gg 1 \quad (3)$$

then three assumptions become valid :

- the jets transport mass and energy instantaneously within the ambient fluid,
- the jet entrainment rate, trajectory and discharge location can be predicted using quasi-steady empirical correlations, without analysis of the detailed transient turbulent transport within the jets, and

- the volume occupied by the jets can be neglected, and the jets can be modeled as line or plane sources and sinks for mass, energy, and species.

Under conditions where the ambient medium stratifies, discussed later, the distribution of mass, energy, and species becomes one-dimensional, and can be described by simple, coupled ordinary differential equations. Stratification can be particularly important when jets originate at intermediate elevations in an enclosure, because the fluid above or below (depending on buoyancy) may not be entrained and mixed, and thus may be effectively isolated.

The product of the residence time and the specific or characteristic frequency gives the specific or characteristic time ratio Π . For the three phase geometries, the time ratios are

$$\Pi_{bj}^s = \omega_{bj}^s \tau_{bj}^s = \frac{u_e n_{bj} A_{bj}}{Q_o} \quad \Pi_{bl}^s = \frac{u_e n_{bl} A_{bl}}{Q_o}$$

$$\Pi_{st} = \frac{\sum_{k=1}^n u_{ek} A_k}{Q_o} = \Pi_{bl}^s + \Pi_{bj}^s. \quad (4)$$

This time ratio characterizes the change in mass, momentum, energy, or species during fluid residence in a jet or ambient volume. Large and small values of the time ratio indicate strong and weak coupling, respectively, and in either case the details of the transport processes become unimportant. Under stratified ambient conditions, large values of the time ratio for jets indicate that the ambient will be well mixed, in the elevation range where the jet takes entrainment. Under unstratified conditions, large values of the time ratio indicate that the entire volume is homogeneously mixed.

3. FREE JETS, WALL JETS, AND AMBIENT FLUID

Here the three regions shown in Fig. 2 (free jets, wall jets, and ambient fluid) are considered. This section uses empirical correlations for jets to derive characteristic entrainment velocities and dimensions. With these quantities, criteria are developed for when buoyancy forces result in strong stratification in the ambient fluid, such that horizontal gradients of temperature and concentration are negligible. Criteria are also derived for assessing the volume occupied by jets relative to the total fluid volume. Finally, simplified governing equations are presented for the stratified ambient transport.

3.1. Forced jets

In large volumes, free buoyant jets can be expected to be turbulent. For turbulent forced jets, List [8] provides an empirical relationship for jet volumetric entrainment rates which is useful for scaling purposes,

$$Q'_{bj} = \frac{dQ_{bj}}{dz} = \frac{Q - Q_o}{H_{st}} = \alpha_T \sqrt{(8\pi M)} \quad (5)$$

where α_T is Taylor's jet entrainment constant, typically taking a value around 0.05, and $M = M_o$ is the momentum of the jet,

$$M_o = \frac{\pi d_{bjo}^2 U_o^2}{4} = \frac{4Q_o^2}{\pi d_{bjo}^2}. \quad (6)$$

For a forced jet the momentum flux is conserved along the path of the jet, such that

$$\frac{M_o}{M} = \frac{U_o Q_o}{U Q} = \frac{U_o^2 d_{bjo}^2}{U^2 d_{bj}^2} = 1. \quad (7)$$

With algebraic manipulation

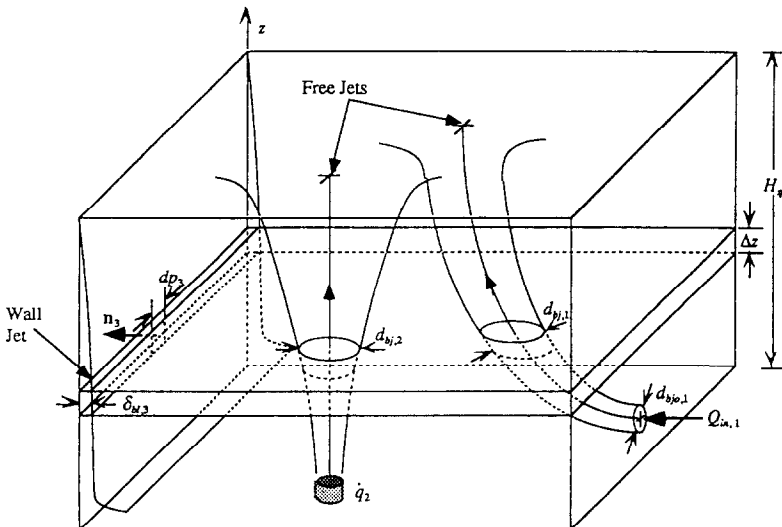


FIG. 2. Schematic of jet discharge in large volume, (1) injected buoyant free jet, (2) buoyant free jet from heat source/sink, and (3) natural convection wall jet.

$$\frac{Q}{Q_o} = 1 + \alpha_T 4\sqrt{2} \left(\frac{H_{sf}}{d_{bjo}} \right) = \frac{d_{bj}}{d_{bjo}} \quad (8)$$

or

$$\frac{d_{bj}}{H_{sf}} = \frac{d_{bjo}}{H_{sf}} + \alpha_T 4\sqrt{2} \quad (9)$$

where d_{bj} is the local lateral spread of the jet. Thus for a turbulent forced jet the jet aspect ratio takes a value independent of Reynolds number, following the common observation that forced jets spread with a constant angle.

For the case of a forced jet, equations (5), (6) and (8) provide the characteristic horizontal velocity generated by entrainment,

$$u_c = \frac{Q'_{bj}}{\pi d_{bj}} = U_o \left(\frac{d_{bjo}}{4H_{sf}} \right) \left(1 + \frac{d_{bjo}}{4\sqrt{2}\alpha_T H_{sf}} \right)^{-1} \quad (10)$$

3.2. Buoyant plumes

Empirical treatments also exist for entrainment into turbulent buoyant plumes. Here we are interested primarily in plumes generated by the injection of a buoyant fluid into a lighter or heavier fluid. The specific buoyancy flux B is related to the densities of the injected fluid and ambient fluid, ρ_o and ρ_a , respectively, and the volume flow rate at the source, Q_o , by

$$B = g \frac{(\rho_a - \rho_o)}{\rho_a} Q_o \quad (11)$$

For a plume generated by a heat source or sink, the buoyancy flux is given by

$$B = \frac{g\beta\dot{q}}{\rho c} \quad (12)$$

where \dot{q} is the heat addition rate, β the fluid thermal expansion coefficient, and c the specific heat.

In an unstratified ambient with constant ρ_a , the inlet buoyancy flux B is conserved along the length of the plume, allowing simplification of the plume analysis and the derivation of relationships for the plume dimensions and entrainment rates. In the enclosure case considered here, the ambient is stratified, in general reducing entrainment. However, for scaling purposes it is still reasonable to use relationships derived for unstratified conditions. For round plumes List [8] gives the local momentum flux as

$$M = k_m B^{2/3} z^{4/3} \quad (13)$$

and the volume flux as

$$Q_{bj} = k_\mu B^{1/3} z^{5/3} \quad (14)$$

Values for the constants k_m and k_μ are approximately 0.35 and 0.15.

The characteristic plume dimension is given by

$$d_{bj} = \frac{Q_{bj}}{M^{1/2}} = \frac{k_\mu}{k_m^{1/2}} z \quad (15)$$

The local volumetric entrainment is given by

$$Q'_{bj} = \frac{5k_\mu}{3} B^{1/3} z^{2/3} \quad (16)$$

A characteristic plume entrainment velocity can then be calculated as

$$u_c = \frac{Q'_{bj}}{\pi d_{bj}} = \frac{5}{3} \left(\frac{1}{2\pi} \right)^{2/3} k_m^{1/2} \left(\frac{g(\rho_a - \rho_o)}{\rho_a} U_o \frac{d_{bjo}^2}{z} \right)^{1/3} \quad (17)$$

3.3. Wall jets

Wall jets form on vertical hot or cold surfaces, due to heat transfer. Both temperature gradients from sensible heat transfer and concentration gradients from condensation with noncondensables present can result in vertical flow and entrainment of ambient fluid, as illustrated in Fig. 2. Characteristic entrainment velocities and dimensions for wall jets are derived here.

Based on an integral solution, Jaluria and Cooper [3] provide useful relationships for turbulent wall boundary layer thickness

$$\frac{\delta_{bl}}{z} = 0.565 \frac{[1 + 0.494 Pr^{2/3}]^{1/10}}{Gr_z^{1/10} Pr^{8/15}} \quad (18)$$

and the characteristic boundary layer velocity

$$\frac{Uz}{\nu} = \frac{1.184 Gr_z^{1/2}}{[1 + 0.494 Pr^{2/3}]^{1/2}} \quad (19)$$

where $Gr_z = g(\rho_a - \rho_o)z^3/\rho_a \nu^2$ is the Grashof number and $Pr = \mu c/k$ the Prandtl number. The integral solution gives the volumetric flow rate at elevation z as

$$\frac{Q_{bj}}{p_{bl}} = 0.1463 U_{bl} \delta_{bl} = \frac{0.0979 \nu Gr_z^{2/5}}{[1 + 0.494 Pr^{2/3}]^{2/5} Pr^{8/15}} \quad (20)$$

where p_{bl} is the wall jet horizontal perimeter. The plume entrainment velocity scale is then

$$u_c = \frac{Q'_{bj}}{p_{bl}} = \frac{0.117 Gr_z^{2/5}}{[1 + 0.494 Pr^{2/3}]^{2/5} Pr^{8/15}} \frac{\nu}{z} \quad (21)$$

3.4. Ambient fluid stratification criteria

The scaling is performed for a large volume enclosure with arbitrary geometry and characteristic height H_{sf} , as shown in Fig. 2. The equations of mass, momentum, energy, and species conservation inside the enclosure are

$$\frac{\partial \rho}{\partial t} + \nabla \cdot (\rho \mathbf{u}) = 0 \quad (22)$$

$$\rho_a \left(\frac{\partial \mathbf{u}}{\partial t} + \nabla \cdot (\mathbf{u} \mathbf{u}) \right) = -\nabla P + \mu \nabla^2 \mathbf{u} - \rho g \mathbf{e}_z \quad (23)$$

$$\frac{\partial \rho i}{\partial t} + \nabla \cdot (\rho i \mathbf{u} - k \nabla T) = 0 \quad (24)$$

$$\frac{\partial \rho \chi_i}{\partial t} + \nabla \cdot (\rho \chi_i \mathbf{u} - \rho D \nabla \chi_i) = 0 \quad (25)$$

where \mathbf{u} is the mass average fluid velocity vector, P the pressure, \mathbf{e}_z the vertical unit vector, i the fluid

enthalpy, T the temperature, and χ_j the mass fraction of species j . The Boussinesq approximation is used for the convective terms of the momentum equations, where the convected density is assumed equal to the nominal ambient density ρ_a . Nondimensional scaling parameters are selected for the enclosure such that the scaled quantities take values of order unity inside the ambient fluid,

$$\mathbf{u}_{sf}^+ = \frac{\mathbf{u}}{u_c} \quad P_{sf}^+ = \frac{(P + \rho_a g z)}{(\rho_a - \rho_o) g H_{sf}} \quad t_{sf}^+ = \frac{t u_c}{H_{sf}}$$

$$\nabla_{sf}^+ = H_{sf} \nabla \quad \rho_{sf}^+ = \frac{\rho - \rho_o}{\rho_a - \rho_o} \quad \theta = \frac{(T - T_o)}{(T_a - T_o)} \quad (26)$$

where u_c is the characteristic radial velocity induced by entrainment in jets.

Now the mass and momentum conservation equations can be written in nondimensional form

$$\frac{\partial \rho_{sf}^+}{\partial t_{sf}^+} + \nabla_{sf}^+ \cdot (\rho_{sf}^+ \mathbf{u}_{sf}^+) = 0 \quad (27)$$

$$\frac{\partial \mathbf{u}_{sf}^+}{\partial t_{sf}^+} + \nabla_{sf}^+ \cdot (\mathbf{u}_{sf}^+ \mathbf{u}_{sf}^+) = - Ri_{e,H_{sf}} \nabla_{sf}^+ P_{sf}^+$$

$$+ \frac{1}{Re_{e,H_{sf}}} \frac{\mu}{\mu_o} \nabla_{sf}^+{}^2 \mathbf{u}_{sf}^+ + Ri_{e,H_{sf}} \rho_{sf}^+ \mathbf{e}_z \quad (28)$$

where the entrainment Richardson and Reynolds numbers are

$$Ri_{e,H_{sf}} = \frac{(\rho_a - \rho_o) g H_{sf}}{\rho_a u_c^2} \quad Re_{e,H_{sf}} = \frac{\rho_a u_c H_{sf}}{\mu_o} \quad (29)$$

Introducing the vorticity,

$$\zeta_{sf}^+ = \nabla_{sf}^+ \times \mathbf{u}_{sf}^+ \quad (30)$$

pressure can be eliminated from the momentum equations, giving the vorticity transport equation,

$$\frac{\partial \zeta_{sf}^+}{\partial t_{sf}^+} + \nabla_{sf}^+ \cdot (\mathbf{u}_{sf}^+ \zeta_{sf}^+) = \frac{1}{Re_{e,H_{sf}}} \frac{\mu}{\mu_o} \nabla_{sf}^+{}^2 \zeta_{sf}^+$$

$$+ Ri_{e,H_{sf}} \nabla_{sf}^+ \rho_{sf}^+ \times \mathbf{e}_z \quad (31)$$

When the entrainment Richardson number is large compared to unity, $Ri_{e,H_{sf}} \gg 1$, and large compared to the inverse Reynolds number, $Ri_{e,H_{sf}} \gg \mu/\mu_o Re_{e,H_{sf}}$, then the vorticity transport equation reduces to the simple form

$$\nabla_{sf}^+ \rho_{sf}^+ \times \mathbf{e}_z \approx 0. \quad (32)$$

Then in the ambient fluid, buoyancy forces cause horizontal density gradients to become negligible, except in narrow regions at the perimeters of free and wall jets. Thus the ambient fluid becomes stratified. In Cartesian coordinates, equation (32) can be written as

$$\frac{\partial \rho}{\partial x} \approx \frac{\partial \rho}{\partial y} \approx 0. \quad (33)$$

For thermal stratification problems, equation (33) requires

$$\frac{\partial T}{\partial x} \approx \frac{\partial T}{\partial y} \approx 0 \quad (34)$$

while for concentration induced stratification it requires

$$\frac{\partial \chi_j}{\partial x} \approx \frac{\partial \chi_j}{\partial y} \approx 0. \quad (35)$$

Under stratified conditions the momentum equation, equation (28), also takes a simplified form,

$$\nabla_{sf}^+ P_{sf}^+ \approx \rho_{sf}^+ \mathbf{e}_z \quad (36)$$

or in dimensional form in Cartesian coordinates,

$$\frac{\partial P_{sf}}{\partial z} \approx -\rho_{sf} g \quad \frac{\partial P_{sf}}{\partial x} \approx \frac{\partial P_{sf}}{\partial y} \approx 0. \quad (37)$$

Using the characteristic horizontal velocity generated by entrainment in a forced jet, equation (10), gives

$$\frac{1}{Re_{e,H_{sf}}} = 4 \frac{\mu_o}{\rho_a U_o d_{bjo}} \left(1 + \frac{d_{bjo}}{4\sqrt{2\alpha_T H_{sf}}} \right) \quad (38)$$

$$Ri_{e,H_{sf}} = 16 \frac{(\rho_a - \rho_o) g H_{sf}}{\rho_a U_o^2} \left(\frac{H_{sf}}{d_{bjo}} \right)^2 \left(1 + \frac{d_{bjo}}{4\sqrt{2\alpha_T H_{sf}}} \right)^2. \quad (39)$$

For a turbulent forced jet it is reasonable to expect that $Re_e, H_{sf} \mu_o/\mu > 1$. Thus the criterion for ambient stratification becomes

$$16 \frac{(\rho_a - \rho_o) g H_{sf}}{\rho_a U_o^2} \left(\frac{H_{sf}}{d_{bjo}} \right)^2 \left(1 + \frac{d_{bjo}}{4\sqrt{2\alpha_T H_{sf}}} \right)^2 \gg 1. \quad (40)$$

Experimental data exist for the breakdown of stable stratification. Using equation (40), one can look for a relationship to correlate the data in the form

$$\frac{H_{sf}}{d_{bjo}} = C \left(\frac{\rho_a U_o^2}{(\rho_a - \rho_o) g d_{bjo}} \right)^{1/3} \left(1 + \frac{d_{bjo}}{4\sqrt{2\alpha_T H_{sf}}} \right)^{2/3}. \quad (41)$$

Jirka [11] correlates stability data by Lee *et al.* [12] and Jain and Balasubramanian [13] in the form

$$\frac{H_{sf}}{d_{bjo}} = 0.22 \left(\frac{\rho_a U_o^2}{(\rho_a - \rho_o) g d_{bjo}} \right)^{1/2}. \quad (42)$$

Figure 3 shows a comparison of equations (41) and (42) with the experimental data. Equation (41), with $C = 1.0$, follows the trend of the stability data better at higher H_{sf}/d_{bjo} values. It is also interesting that the data for stability of nonvertical injection are also correlated reasonably well by equation (41). The stability data were generated in shallow water layers. Because the recirculation patterns which result after the breakdown of stratification are three-dimensional, for enclosures the breakdown of stratification will be modified somewhat.

With $C = 1.0$ equation (41) provides criteria for when an injected jet will not cause break down of stratification in an enclosure.

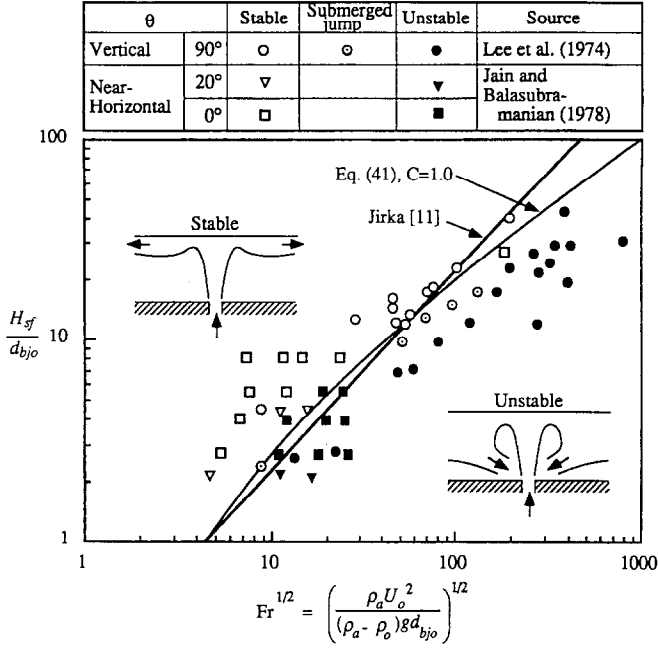


FIG. 3. Stability criterion for round free buoyant jets.

$$\left(\frac{H_{sf}}{d_{bj0}} \right) Ri_{d_{bj0}}^{1/3} \left(1 + \frac{d_{bj0}}{4\sqrt{2}\alpha_T H_{sf}} \right)^{2/3} > 1 \quad (43)$$

where the jet Richardson number is given by

$$Ri_{d_{bj0}} = \frac{(\rho_a - \rho_o) g d_{bj0}}{\rho_a U_o^2}. \quad (44)$$

For the buoyant plume case the local velocity scale comes from equation (17) and

$$\frac{1}{Re_{c,H_{sf}}} = \frac{2.04}{k_m^{1/2}} \left(\frac{\rho_a U_o^2}{g(\rho_a - \rho_o) d_{bj0}} \right)^{1/3} \left(\frac{H_{sf}}{d_{bj0}} \right)^{1/3} \frac{\mu_o}{\rho_a U_o H_{sf}} \quad (45)$$

$$Ri_{c,H_{sf}} = \frac{4.17}{k_m} \left(\frac{g(\rho_a - \rho_o) d_{bj0}}{U_o^2 \rho_a} \right)^{1/3} \left(\frac{H_{sf}}{d_{bj0}} \right)^{5/3}. \quad (46)$$

Thus for a buoyant plume when

$$\frac{4.17}{k_m} \left(\frac{H_{sf}}{d_{bj0}} \right)^{5/3} Ri_{d_{bj0}}^{1/3} \gg 1 \quad (47)$$

horizontal density gradients in the ambient fluid become negligible. Gebhart *et al.* [9] give the length scale for the location of the transition from forced jet to buoyant plume for cylindrical buoyant jets, z_{trans} ,

$$\left(\frac{\rho_o U_o^2}{(\rho_a - \rho_o) g d_{bj0}} \right)^{-1/4} \left(\frac{\rho_o}{\rho_a} \right)^{-1/4} \left(\frac{z_{trans}}{d_{bj0}} \right) = 1. \quad (48)$$

Then equation (47) can be written as

$$\frac{4.17}{k_m} \left(\frac{H_{sf}}{d_{bj0}} \right)^{1/3} \left(\frac{H_{sf}}{z_{trans}} \right)^{4/3} \left(\frac{\rho_o}{\rho_a} \right)^{2/3} \gg 1. \quad (49)$$

Because $H_{sf} > z_{trans}$, the criterion for stratification of

the ambient is almost always satisfied for turbulent buoyant plumes.

For turbulent wall jets, equation (21) gives the characteristic entrainment velocity, and

$$\frac{1}{Re_{c,H_{sf}}} = 8.55 \frac{[1 + 0.494 Pr^{2/3}]^{2/5} Pr^{8/15}}{Gr_{H_{sf}}^{2/5}} \quad (50)$$

$$Ri_{c,H_{sf}} = 73.1 [1 + 0.494 Pr^{2/3}]^{4/5} Pr^{16/15} Gr_{H_{sf}}^{1/5}. \quad (51)$$

Thus for a wall jet when

$$73.1 [1 + 0.494 Pr^{2/3}]^{4/5} Pr^{16/15} Gr_{H_{sf}}^{1/5} \gg 1 \quad (52)$$

then horizontal density gradients in the ambient fluid become negligible. For vertical surfaces over 1 m in height with typical temperature and concentration differences between surfaces and ambient fluids, the criterion for stratification is almost always satisfied.

3.5. Ambient fluid energy and species transport

Next the energy equation in the ambient fluid can be examined, integrating over a thin horizontal volume V with height Δz and area $A_s(z)$, as shown in Fig. 2,

$$\int_V \left[\frac{\partial \rho i}{\partial t} + \nabla \cdot (\rho i \mathbf{n} - k \nabla T) \right] dV = 0. \quad (53)$$

Applying Gauss' theorem, this can be written as

$$\frac{\partial}{\partial t} \int_V \rho i dV + \int_S [\mathbf{n} \cdot (\rho i \mathbf{n} - k \nabla T)] dS = 0 \quad (54)$$

where \mathbf{n} is the unit normal vector to surface S which bounds volume V . Summing over the top and bottom surfaces, and the various free and wall jet surfaces

$k = 1$ to n with perimeters p_k and height Δz which bound V , equation (54) becomes

$$\begin{aligned} \hat{c} \int_z^{z+\Delta z} \int_{A_{sf}(z)} \rho i \, dA \, dz + \int_{A_{sf}(z+\Delta z)} [\mathbf{e}_z \cdot (\rho i \mathbf{u} - k \nabla T)] \, dA \\ - \int_{A_{sf}(z)} [\mathbf{e}_z \cdot (\rho i \mathbf{u} - k \nabla T)] \, dA \\ + \sum_{k=1}^n \left\{ \int_z^{z+\Delta z} \int_0^{p_k} [\mathbf{n} \cdot (\rho i \mathbf{u})] \, dp_k \, dz \right\} = 0. \quad (55) \end{aligned}$$

The diffusion term is dropped from the jet surface entrainment terms, because scaling shows it is small compared to convection for turbulent jets. However, the diffusion term is kept for the horizontal surfaces, because under transient conditions where the jet flow rates drop to very low values, then molecular diffusion becomes a significant mechanism for vertical energy and species redistribution. Noting that under stratified conditions equations (33) and (34) give $\rho = \rho(z, t)$ and $T_{sf} = T_s(z, t)$, respectively (except in narrow regions at the perimeter of jets, where the horizontal gradients of ρ and T_{sf} can become significant), then for small Δz

$$\begin{aligned} A_{sf}(z) \Delta z \frac{\partial \rho i_{sf}}{\partial t} + (\rho i_{sf} Q_{sf})_{(z+\Delta z)} - (\rho i_{sf} Q_{sf})_{(z)} + A_{sf}(z) \\ \times \left[\left(k \frac{\partial T_{sf}}{\partial z} \right)_z - \left(k \frac{\partial T_{sf}}{\partial z} \right)_{z+\Delta z} \right] + \sum_{k=1}^n (\rho i_k \delta Q_k) = 0 \quad (56) \end{aligned}$$

where the vertical volume flow rate is

$$Q_{sf}(z) = \int_{A_{sf}(z)} [\mathbf{e}_z \cdot \mathbf{u}] \, dA \quad (57)$$

and the entrainment rate in jet k is

$$\frac{\delta Q_k}{\Delta z} = Q'_k = \int_0^{p_k} [\mathbf{n} \cdot \mathbf{u}] \, dp_k. \quad (58)$$

The enthalpy i_k is determined in an upwind manner, so that

$$\begin{aligned} i_k = i_{sf}(z) \quad \delta Q_k \geq 0 \quad (\text{jet entrainment}) \\ i_k = i_j(z) \quad \delta Q_k < 0 \quad (\text{jet discharge}) \quad (59) \end{aligned}$$

where the jet discharge enthalpy i_j is

$$i_j = \frac{\int_0^{H_{sf}} \rho_{sf} i_{sf} Q'_k \, dz}{\int_0^{H_{sf}} \rho_{sf} Q'_k \, dz}. \quad (60)$$

Dividing and taking the limit as $\Delta z \rightarrow 0$ the ordinary differential equation is obtained from equation (56),

$$\begin{aligned} A_{sf}(z) \frac{\partial \rho i_{sf}}{\partial t} + \frac{\partial}{\partial z} \left(\rho i_{sf} Q_{sf} - A_{sf}(z) k \frac{\partial T_{sf}}{\partial z} \right) \\ + \sum_{k=1}^n (\rho i_k Q'_k) = 0. \quad (61) \end{aligned}$$

The species transport equation, equation (25), can be reduced in the same way to the form of equation (61).

3.6. Ratio of jet volumes to ambient fluid volume

When the volume occupied by jets is small compared to the ambient fluid volume, then the details of the temperature and species distributions inside the jets can be neglected, and the material in the jets can be lumped with the ambient fluid, $A_{sf} = A$. Fluid particle residence time in the jets can also be neglected, and the jets can be assumed to instantaneously transport fluid from the entrainment elevation to the jet discharge elevation. For forced jets, the residence time ratio, equation (3), can be found using equation (9)

$$\frac{\tau_{sf}}{\tau_{bj}^s} = \frac{V_{sf}}{n_{bj} V_{bj}} = \frac{4}{\pi} \frac{V_{sf}}{H_{bj}^3 n_{bj}} \left(\frac{d_{bjo}}{H_{bj}} + \alpha_T 4\sqrt{2} \right)^{-2}. \quad (62)$$

Because $(\alpha_T 4\sqrt{2})^{-2} \approx 12$, the scaling is nominally satisfied when $V_{sf}/H_{bj}^3 n_{bj} > 1$.

For buoyant plumes, using equation (15),

$$\frac{\tau_{sf}}{\tau_{bj}^s} = \frac{V_{sf}}{n_{bj} V_{bj}} = \frac{4}{\pi} \frac{V_{sf}}{H_{bj}^3 n_{bj}} \left(\frac{k_m}{k_\mu^2} \right). \quad (63)$$

Because $k_m/k_\mu^2 \approx 16$, the scaling is nominally satisfied when $V_{sf}/H_{bj}^3 n_{bj} > 1$.

For wall jets, using equations (19) and (20), the ratio of residence times is

$$\frac{\tau_{sf}}{\tau_{bl}^s} = \frac{V_{sf}/n_{bl} Q_{bl}}{H_{bl}/U_{bl}} = 12.1 \frac{V_{sf}}{H_{bl}^2 n_{bl} \rho_{bl}} \frac{Gr_{bl}^{1/10} Pr^{8/15}}{[1 + 0.494 Pr^{2/3}]^{1/10}}. \quad (64)$$

The relative residence time in wall boundary layers then depends on the wall perimeter and height, and the Grashof and Prandtl numbers.

3.7. Governing equations for the stratified ambient fluid

For the stratified enclosure, the governing equations can then be written in the following compact form,

$$A(z) \frac{\partial \mathbf{G}}{\partial t} + \frac{\partial \mathbf{F}}{\partial z} = \mathbf{S} \quad (65)$$

where $A(z)$ is the horizontal cross sectional area of the volume at elevation z , and \mathbf{G} , \mathbf{F} , and \mathbf{S} are the vectors of conserved quantities, fluxes, and source terms respectively,

$$\mathbf{G} = \begin{bmatrix} \rho \\ 0 \\ \rho i \\ \rho \chi_1 \\ \vdots \\ \rho \chi_{ns-1} \end{bmatrix} \quad \mathbf{F} = \begin{bmatrix} \rho Q_{sf} \\ P \\ \rho i Q_{sf} - Ak \frac{\partial T_{sf}}{\partial z} \\ \rho \chi_1 Q_{sf} - \rho AD \frac{\partial \chi_1}{\partial z} \\ \vdots \\ \rho \chi_{ns-1} Q_{sf} - \rho AD \frac{\partial \chi_{ns-1}}{\partial z} \end{bmatrix}$$

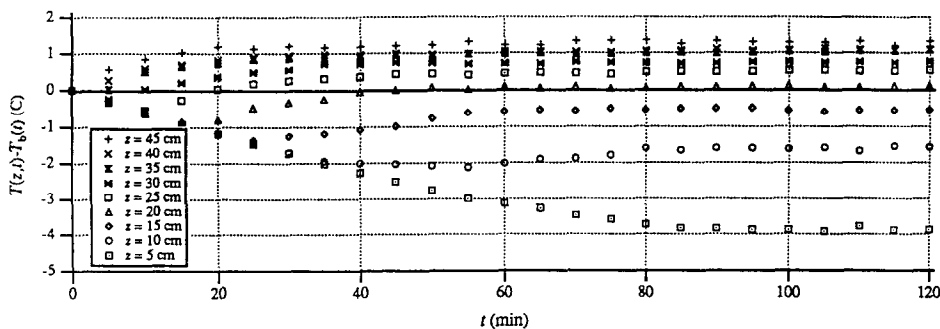


FIG. 4. Transient experimental temperature distribution in a heated pool [4].

$$S = \begin{pmatrix} \sum_{k=1}^n (\rho Q')_k \\ -\rho g \\ \sum_{k=1}^n (\rho i Q')_k \\ \sum_{k=1}^n (\rho \chi_1 Q')_k \\ \vdots \\ \sum_{k=1}^n (\rho \chi_{n-1} Q')_k \end{pmatrix} \quad (66)$$

4. APPLICATIONS

The one-dimensional governing equations, equations (66), can be solved numerically using explicit finite difference methods. Fox *et al.* [4] performed such an analysis for an immersed heat source. The analysis was compared to experiments which used a 1.35 kW, 15 cm tall electric resistance heater. The bottom of the heater was submerged at a 50 cm depth in a 2 m high, 95 cm diameter tank. Their experiment found strong thermal stratification above the base of the heater, with a vertical thermocouple rake measuring negligible horizontal temperature changes when moved, except in the region near the thermal plume. No measurable heat propagation was observed below the heater. Heat loss from the fiberglass tank walls was calculated to be negligible, however, heat loss from the pool surface was up to 10% of the input power. Figure 4 shows their experimental data, plotted as the

difference between the local temperature and the bulk temperature of the water layer above the heater. At long times the temperature distribution in the surface layer approached a quasi-steady condition.

Fox *et al.* [4] modeled the experimental system using governing equations, equations (66). The plume correlation equation (14) with $k_\mu = 0.148$ was used to determine the axial entrainment rate in the plume. They assumed that the plume discharged at the surface, spreading as an infinitesimally thin layer. Figure 5 shows the numerical results. The model predicts that a sharp temperature front propagates downward in the pool. The experiments show that the front is more diffuse, due to the finite thickness of the spreading layer at the surface. However, the long term temperature distribution was well predicted. Also, as was observed experimentally, the model predicted no propagation of heat below the base of the heater.

5. CONCLUSIONS

When the ambient fluid in a large enclosure stratifies, the temperature and species distributions become one-dimensional and can be modeled by simple governing equations, equations (66), using standard empirical relationships for jet entrainment. The detailed geometry of the enclosure becomes unimportant, and only the horizontal cross-sectional area and perimeter must be specified as a function of elevation. This allows very large reductions in computational effort compared to three-dimensional

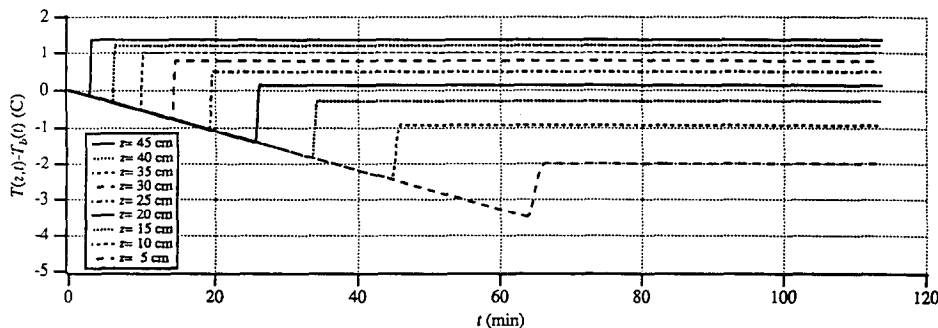


FIG. 5. Transient numerical simulation of temperature distributions in a heated pool [4].

numerical modeling of turbulent mixing in large enclosures. Large enclosures mixed by buoyant plumes and wall jets can normally be expected to stratify. The momentum injected by forced jets can potentially break down stratification in large enclosures; equation (43) provides a criteria for assessing when breakdown will occur.

REFERENCES

1. Y. Jaluria, Buoyancy driven wall flows in enclosure fires, *Twenty-first Symposium (International) on Combustion*, The Combustion Institute, pp. 151–157 (1986).
2. D. Goldman and Y. Jaluria, Effect of opposing buoyancy on the flow in free and wall jets, *J. Fluid Mech.* **166**, 41–56 (1986).
3. Y. Jaluria and L. Y. Cooper, Negatively buoyant wall flows generated in enclosure fires, *Prog. Energy Combust. Sci.* **15**, 159–182 (1989).
4. R. J. Fox, D. B. McDonald, P. F. Peterson and V. E. Schrock, Temperature distribution in pools with shallow buoyant jets, *Fifth International Topical Meeting on Nuclear Reactor Thermal Hydraulics (NURETH-5)*, 21–24 September, Salt Lake City, Utah, Vol. 4, pp. 1227–1234 (1992).
5. B. L. Smith, T. V. Dury, M. Huggenberger and H. Nöthinger, Analysis of single-phase mixing experiments in open pools, *Thermal Hydraulics of Advanced and Special Purpose Reactors* (Edited F. B. Cheung and P. F. Peterson), ASME HTD-Vol. 209, pp. 91–100. New York (1992).
6. P. F. Peterson, V. E. Schrock and R. Greif, Scaling for integral simulation of mixing in large, stratified volumes, *Sixth International Topical Meeting on Nuclear Reactor Thermal Hydraulics (NURETH-6)*, 5–8 October, Grenoble, France, Vol. 1, pp. 202–211 (1993).
7. C. J. Chen and W. Rodi, *Vertical Turbulent Jets: A Review of Experimental Data*, Pergamon Press, New York (1980).
8. E. J. List, Mechanics of turbulent buoyant jets and plumes. In *Turbulent Buoyant Jets and Plumes* (Edited by W. Rodi), Pergamon Press, New York (1982).
9. B. Gebhart, Y. Jaluria, R. L. Mahajan and B. Sammakia, *Buoyancy-Induced Flows and Transport*, Hemisphere, New York (1988).
10. N. Zuber, An integrated structure and scaling methodology for severe accident technical issue resolution, Appendix D, NUREG/CR-5809, U.S. Nuclear Regulatory Commission (1991).
11. G. H. Jirka, Turbulent buoyant jets in shallow fluid layers. In *Turbulent Buoyant Jets and Plumes* (Edited by W. Rodi), Pergamon Press, New York (1982).
12. J. H. Lee, G. H. Jirka and D. R. F. Harleman, Stability and mixing of a vertical round buoyant jet in shallow water, M.I.T., Ralph M. Parsons Laboratory for Water Resources and Hydrodynamics, Tech. Rep. No. 195 (1974).
13. S. C. Jain and V. Balasubramanian, Horizontal buoyant jets in quiescent shallow water, *J. Environ. Engng Div., Proc. A.S.C.E.* **104**, EE4 (1978).